

# Characterization and CO Oxidation Activity Studies of Co-Based Catalysts

Filiz BALIKÇI<sup>1</sup>, Çiğdem GÜLDÜR<sup>2\*</sup>

<sup>1</sup>*Gazi University, Institute of Science and Technology, Ankara-TURKEY*

<sup>2</sup>*Gazi University, Faculty of Engineering and Architecture, Chemical Engineering Department, Ankara-TURKEY*

*e-mail: cguldur@gazi.edu.tr*

Received 22.03.2007

Cobalt oxide based catalysts were developed for carbon monoxide oxidation at low temperature. The catalysts were prepared by co-precipitation and calcined at 200 °C. Several techniques were used to characterize the catalysts, such as X-ray diffractometer system, N<sub>2</sub> physisorption measurements, scanning electron microscope (SEM), and X-ray photoelectron spectroscopy. Carbon monoxide oxidation studies were carried out to investigate the relation between the characteristic properties of the catalysts and the catalytic activity. Catalytic activity measurements were studied from room temperature to 200 °C, using a feed composition of 1% CO, 21% O<sub>2</sub>, and remaining He. X-ray studies showed that the catalysts have an amorphous phase structure. The average pore diameter of the catalysts was in the mesopore diameter range. The pore sizes and pore volumes of the catalysts increased with increasing molar ratio of cobalt oxide in the catalysts. BET surface areas of the catalysts mostly depend on the cobalt oxide molar ratio in the structure of the catalysts. Low temperature CO oxidation activity measurements showed that the best activity was obtained from the 50/50 Co<sub>3</sub>O<sub>4</sub>/CeO<sub>2</sub> catalyst, which has the light of temperature around 122 °C and yielded 100% CO conversion above 160 °C.

**Key Words:** Cobalt oxide, cerium, silver oxide, CO oxidation, characterization.

## Introduction

The oxidation of carbon monoxide is a very important reaction, and low temperature carbon monoxide oxidation reaction catalysts are important in many applications. Low temperature CO oxidation catalysts are used in residential and automotive air cleaning technologies, gas masks for mining applications, CO detectors, and selective oxidation of CO in reformer gas for fuel cell applications. Research interest in the catalytic oxidation of carbon monoxide has surged because of the possible uses for air cleaning, orbiting, closed-cycle CO<sub>2</sub> lasers, and other remote sensing applications. Characteristic properties of a catalyst and pretreatment conditions have an effect on the catalytic activity of catalysts. Metal oxide catalysts are preferred for carbon monoxide oxidation reactions. Cobalt oxide based catalysts are used for ethanol steam

---

\*Corresponding author

reforming, oxidation of methane, Fischer-Tropsch synthesis, CO-NO reactions, carbon monoxide oxidation, and pyridine oxidation.<sup>1–5</sup> Different promoters are added to the catalyst structure to investigate the effect of the promoters on the activity of the cobalt oxide catalysts.<sup>6,7</sup> Cerium oxide has been widely used as an oxygen storage medium and as a thermal stabilizer. The promoting roles of ceria are proposed to involve multiple processes such as the enhancement of the noble metal dispersion and the stabilization of the support toward thermal sintering.<sup>6</sup> Previous studies investigated the effect of the impurities present in the exhaust emissions on the CO oxidation activity. The CO oxidation was inhibited by these compounds and the main reason for the loss of activity when different compounds are added to the gas phase mixture is suggested to originate from their adsorption and the formation of different species on the cobalt oxide surface.<sup>7</sup>

The aim of this study was to investigate the effect of cerium oxide and silver oxide on the characteristic properties and low temperature CO oxidation activity of cobalt oxide catalysts. Three different catalysts, namely  $\text{Co}_3\text{O}_4$ , 50/50  $\text{Co}_3\text{O}_4/\text{CeO}_2$ , and 25/25/50  $\text{Ag}_2\text{O}/\text{Co}_3\text{O}_4/\text{CeO}_2$ , were investigated. Several techniques were used to characterize the catalysts and low temperature CO oxidation activities of the catalysts were investigated. Some characterization and catalytic activity results of pure oxide catalysts ( $\text{Ag}_2\text{O}$ ,  $\text{Co}_3\text{O}_4$ , and  $\text{CeO}_2$ ) are not represented here.

## Experimental

The catalysts were prepared by co-precipitation as single oxide catalysts and at different metal/metal oxide molar ratios.  $\text{AgNO}_3$  (Aldrich, 99.8%),  $\text{Co}(\text{NO}_3)_2 \cdot 6\text{H}_2\text{O}$  (Fluka, 99.0%), and  $\text{CeN}_3\text{O}_9 \cdot 6\text{H}_2\text{O}$  (Sigma, 99%) at desired molar ratios were dissolved in distilled water. The total concentration of the metals in the combined aqueous solutions was 0.1 M. The metal salt solution was placed in a stirrer.  $\text{Na}_2\text{CO}_3$  (1 M) solution was added to the metal salt solution to adjust the pH of the solution to 8. The precipitates were aged for 3 h at pH 8 and filtered and washed with hot distilled water several times to remove excess ions. They were dried in air at 110 °C overnight. The catalysts were calcined in air at 200 °C for 3 h.

X-ray diffraction (XRD) was used to identify the phases present in the synthesized samples. A Rigaku rotating anode X-ray diffractometer system generating  $\text{CuK}\alpha$  radiation was used to obtain the XRD patterns.

Surface areas and pore volumes of the catalysts were determined by nitrogen adsorption on a Quantachrome Autosorb 1C system. The samples were kept at 200 °C under vacuum before starting  $\text{N}_2$  adsorption at liquid temperature. Calculation of pore sizes followed the Barrett-Joyner-Halenda (BJH) method according to the implemented software routines using the Halsey thickness equation to relate the thickness of the adsorbed layer to the relative pressure. All calculations are based on the desorption model.

XPS analyses were performed with a SPECS SAGE-150 spectrometer, using  $\text{MgK}\alpha$  radiation (1486.6 eV) operating at an accelerating voltage of 12.5 kV. Charging effects were corrected by adjusting the C 1s peak to a position of 284.5 eV. The samples were pressed into thin disks and mounted on a sample rod placed in a pretreatment chamber. The spectra of Ag 3d, Co 2p, O 1s, and Ce 3d levels were recorded.

Catalyst morphology was examined using a JEOL/JSM-6335F scanning electron microscope. The electron gun was operated at an accelerating voltage of 12 kV to collect all images.

Catalytic activity measurement was carried out in a fixed bed quartz tube reactor using 25–35 mg catalyst. The flow rate of the feed gas was 25 mL/min. The reactant gas consisted of 1(vol.)%  $\text{CO}$ , 21(vol.)%  $\text{O}_2$ , and remaining He was passed through the catalyst bed. Activity measurements were carried out at different temperatures in the range of 20–200 °C. The analysis of the reactor effluent was performed

with an on-line Perkin Elmer CLARUS 500 gas chromatograph with a thermal conductivity detector (TCD). The chromatograph column's packing was carbosphere and the column temperature was maintained at 50 °C (The catalytic activity system shown in Güldür et al.<sup>8</sup> was used).

## Results and Discussion

X-ray diffraction studies were carried out to see the phases present in the catalysts. The catalysts showed different phase structures. It was determined that the calcination temperature is very effective on the phases. Both 50/50 Co<sub>3</sub>O<sub>4</sub>/CeO<sub>2</sub> and 25/25/50 Ag<sub>2</sub>O/Co<sub>3</sub>O<sub>4</sub>/CeO<sub>2</sub> catalysts have amorphous phase structures. The single cobalt oxide catalyst showed peaks due to the Co<sub>3</sub>O<sub>4</sub> phase.

N<sub>2</sub> physisorption measurements were obtained to investigate the adsorption/desorption behaviors, BET surface areas, pore volumes, and average pore diameters of the catalysts. All values were obtained by Quantachrome Autosorb 1C instrument. Figure 1 shows the adsorption-desorption isotherms of the catalysts and Table 1 shows the physical properties of the catalysts. The adsorption-desorption isotherms fit the Type V isotherm in the BDDT classification. One of the characteristic features of the isotherms in the BDDT classification is the hysteresis loop. The pore volume and the width of the hysteresis loop increased correspondingly with the increase in Co<sub>3</sub>O<sub>4</sub> molar ratio. The area under the hysteresis loop is related to the BET surface areas of the catalysts. Moreover, it is directly proportional to the surface area. The area of the hysteresis loop increases with the increase in cobalt oxide molar ratio. All catalysts presented large surface areas. The surface area of the cobalt oxide catalyst was decreased when CeO<sub>2</sub> or Ag<sub>2</sub>O was added to the catalyst structure. The decreasing effect of Ag<sub>2</sub>O was greater than that of CeO<sub>2</sub>. The decrease in the surface area value was considerably apparent when the Co<sub>3</sub>O<sub>4</sub> molar ratio was decreased. All catalysts had average pore diameters between 2 and 50 nm. Pore diameters of the catalysts changed in a very wide range. None of the 3 catalysts yielded the same average pore diameter. The average pore diameters of the 3 catalysts was centered at 2.2 nm; and the 100% Co<sub>3</sub>O<sub>4</sub> and 50/50 Co<sub>3</sub>O<sub>4</sub>/CeO<sub>2</sub> catalysts have second average pore diameters of 18 nm and 24 nm, respectively. The variable pore structure of the cobalt oxide phase has an increasing effect on the average pore diameter of the other catalysts. This property has also an effect on the pore volume and BET surface areas of the catalysts. Bigger average pore diameters obtained from the catalysts were supported by Kang et al.,<sup>6</sup> who found that 15/75 Co<sub>3</sub>O<sub>4</sub>/CeO<sub>2</sub> catalysts calcined at 550 °C have a 14.4 nm average pore diameter. The small difference between the 2 studies is mainly due to the calcination temperature and metal oxide molar ratio. The total pore volume of the 25/25/50 Ag<sub>2</sub>O/Co<sub>3</sub>O<sub>4</sub>/CeO<sub>2</sub> catalyst is approximately 20% smaller than the total pore volume of the 50/50 Co<sub>3</sub>O<sub>4</sub>/CeO<sub>2</sub> catalyst. The difference is due to the change in the cobalt oxide molar ratio in the structures of the catalysts. The pore volume results of the catalysts showed that most of the pore volume was a composition of mesopores. The catalysts had a very small micropore volume in comparison with the mesopores. The total pore volumes of the catalysts were decreased by the addition of Ag<sub>2</sub>O to the catalysts.

The change in the pore sizes and shapes could be seen in the scanning electron microscopy photographs (Figure 2). The catalysts had uniform particles and the shape of the particles was spherical. The sizes of the agglomerates were uniform and the gaps between the agglomerates were small for the 50/50 Co<sub>3</sub>O<sub>4</sub>/CeO<sub>2</sub> catalysts. Addition of the Ag<sub>2</sub>O phase to the structure of the Co<sub>3</sub>O<sub>4</sub>/CeO<sub>2</sub> catalyst affected the shape of the agglomerates. The gaps between the agglomerates increased and the size of the agglomerates changed in the 25/25/50 Ag<sub>2</sub>O/Co<sub>3</sub>O<sub>4</sub>/CeO<sub>2</sub> catalysts.

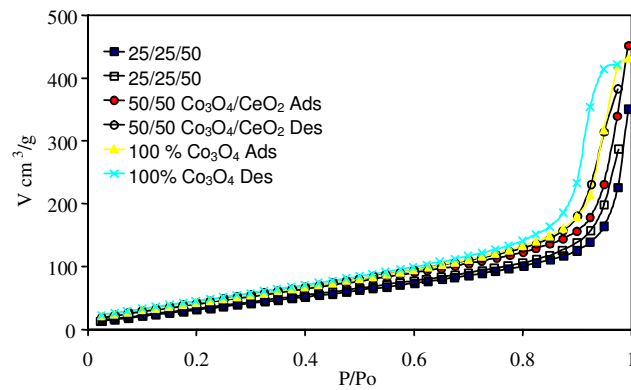
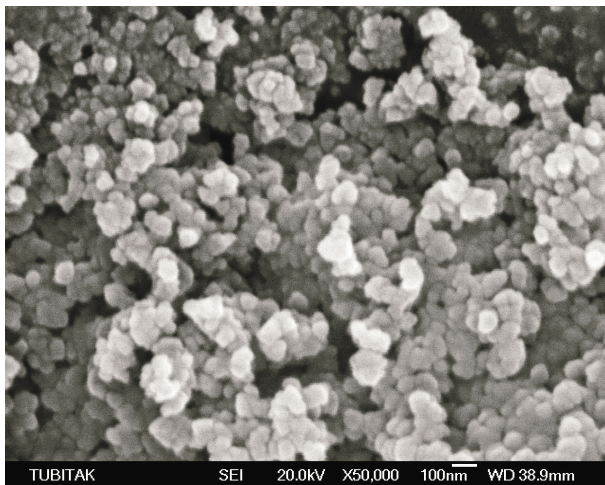


**Figure 1.** N<sub>2</sub> adsorption/desorption isotherms of the catalysts.

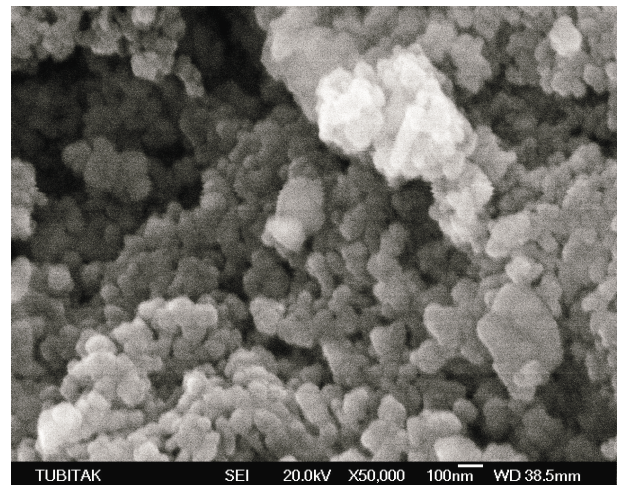
**Table 1.** The characteristic properties of the catalysts obtained from the N<sub>2</sub> physisorption measurements.

Catalysts	BET Surface Areas m <sup>2</sup> /g	Micro Pore Volume V[=] liquid N <sub>2</sub> volume cm <sup>3</sup> /g	Meso Pore Volume V[=] liquid N <sub>2</sub> volume cm <sup>3</sup> /g	Average Pore Diameter nm
100 % Co <sub>3</sub> O <sub>4</sub>	185.2	0.009	0.66	2.2, 18*
50/50 Co <sub>3</sub> O <sub>4</sub> /CeO <sub>2</sub>	180.3	0.008	0.66	2.2, 14*
25/25/50 Ag <sub>2</sub> O/Co <sub>3</sub> O <sub>4</sub> /CeO <sub>2</sub>	148.0	0.005	0.50	2.2

\*Catalysts gave 2 average pore diameters



(A)



(B)

**Figure 2.** Scanning electron microscopy photograph of 50/50 Co<sub>3</sub>O<sub>4</sub>/CeO<sub>2</sub> (A) and 25/25/50 Ag<sub>2</sub>O/Co<sub>3</sub>O<sub>4</sub>/CeO<sub>2</sub> (B).

X-ray photoelectron spectroscopy was used to see the oxidation state of the catalysts calcined at 200 °C, since these catalysts showed an amorphous structure in the X-ray diagram. Figure 3 shows the XPS spectrum of the 50/50 Co<sub>3</sub>O<sub>4</sub>/CeO<sub>2</sub> and 25/25/50 Ag<sub>2</sub>O/Co<sub>3</sub>O<sub>4</sub>/CeO<sub>2</sub> catalysts. The Ag 3d<sub>5/2</sub> binding energy of the 25/25/50 Ag<sub>2</sub>O/Co<sub>3</sub>O<sub>4</sub>/CeO<sub>2</sub> catalyst is 369.08 eV. The Ag3d peak can be compared with 367.3 eV for Ag<sub>2</sub>CO<sub>3</sub>, 367.7 eV for Ag<sub>2</sub>O, 367.8 for AgO eV, and 368 eV for Ag/Al<sub>2</sub>O<sub>3</sub>.<sup>9–11</sup> The Co2p<sub>1/2</sub> binding energies of the 50/50 Co<sub>3</sub>O<sub>4</sub>/CeO<sub>2</sub> and 25/25/50 Ag<sub>2</sub>O/Co<sub>3</sub>O<sub>4</sub>/CeO<sub>2</sub> catalysts are 794.58 eV and

796.5 eV, respectively. The Co 2p peaks can be compared with 779.4 eV for  $\text{Co}_3\text{O}_4$  in Cu-Co oxide and 779.9 eV for  $\text{Co}_3\text{O}_4$  in  $\text{Co}_3\text{O}_4$  catalysts.<sup>12,13</sup> The O1s binding energies of the 50/50  $\text{Co}_3\text{O}_4/\text{CeO}_2$  and 25/25/50  $\text{Ag}_2\text{O}/\text{Co}_3\text{O}_4/\text{CeO}_2$  catalysts are 528.97 eV and 530.78 eV, respectively. The O 1s peaks can be compared with 532.1 eV and 529.2 eV in  $\text{Ag}_2\text{O}$  catalysts, 529.7 eV in  $\text{Co}_3\text{O}_4$  catalysts, and 529.4 eV in  $\text{CeO}_2$  catalysts.<sup>10,11,13,14</sup> The  $\text{Ce}3d_{5/2}$  binding energy of the 50/50  $\text{Co}_3\text{O}_4/\text{CeO}_2$  catalyst is 881.97 eV, 887.81 eV, and 897.79 eV. The  $\text{Ce}3d_{5/2}$  binding energy of the 25/25/50  $\text{Ag}_2\text{O}/\text{Co}_3\text{O}_4/\text{CeO}_2$  catalyst is 883.75 eV, 890.88 eV, 900 eV, and 902.31 eV. The  $\text{Ce}3d_{3/2}$  peak has a binding energy of 916.04 eV in the 50/50  $\text{Co}_3\text{O}_4/\text{CeO}_2$  catalyst and 918.03 eV in the 25/25/50  $\text{Ag}_2\text{O}/\text{Co}_3\text{O}_4/\text{CeO}_2$  catalyst. The Ce 3d peaks can be compared with 916.8 eV for Ce(IV) and 882.6 eV for Ce(III); 883.0 eV, 889.6 eV, 899 eV, 901.2 eV, 908 eV, and 917 eV for Ce(IV) in  $\text{CeO}_2$  catalysts.<sup>15,16</sup> The peaks observed in the XPS measurements are consistent with the reference studies. According to these results, oxidation states of silver, cobalt, and ceria are +1, +3, and +4, respectively.

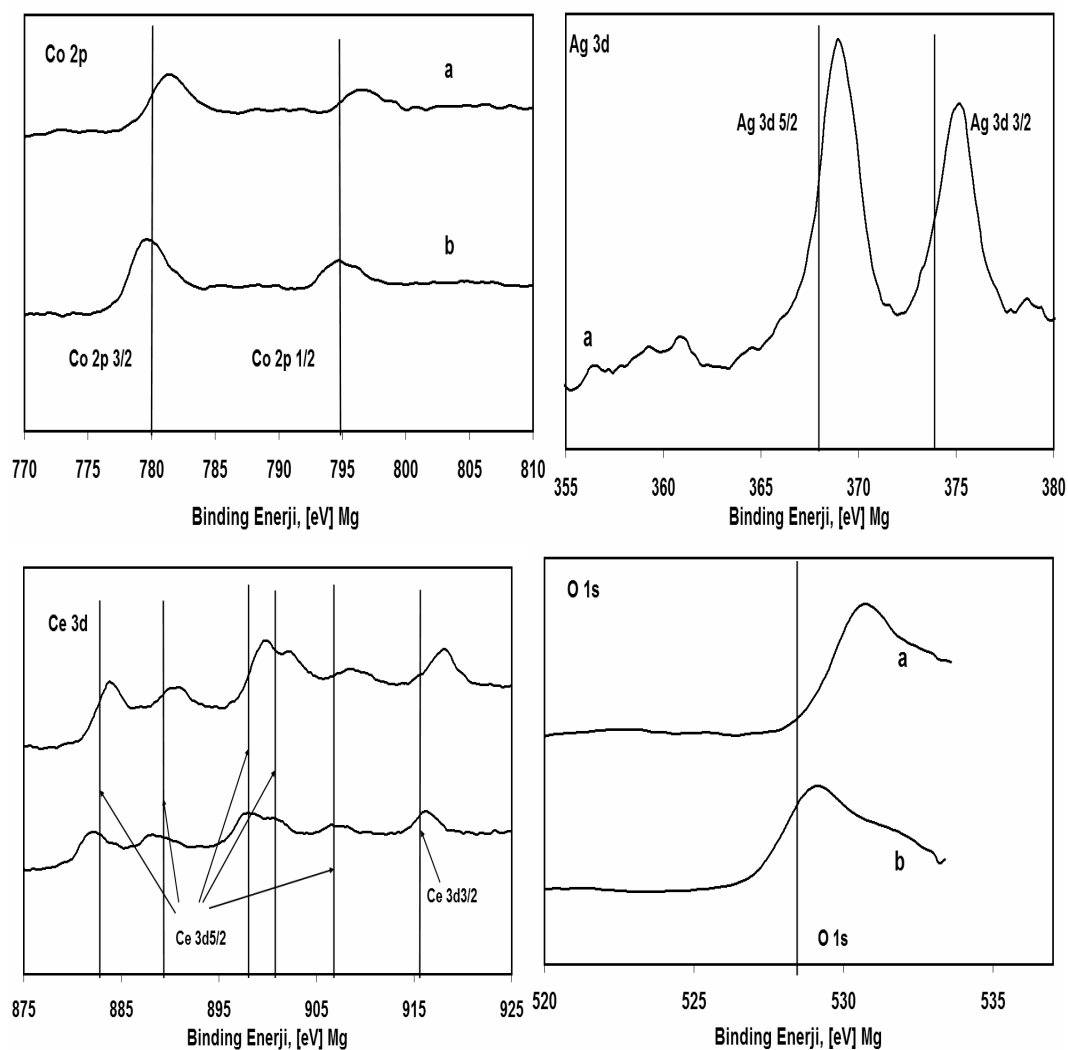


**Figure 3.** XPS spectrum of the catalysts (a: 25/25/50  $\text{Ag}_2\text{O}/\text{Co}_3\text{O}_4/\text{CeO}_2$  and b: 50/50  $\text{Co}_3\text{O}_4/\text{CeO}_2$ ).

Low temperature carbon monoxide oxidation activities of the catalysts were investigated with 1% CO, 21% O<sub>2</sub>, and remaining He gas mixtures between room temperature and 200 °C. Figure 4 shows the % CO conversion as a function of temperature and Table 2 shows the 50% and 100% temperatures of the catalysts. The catalytic activity of the catalysts is related to the light of temperature, which is the 50% conversion temperature of the catalyst. The smallest light of temperature shows the highest catalytic activity. The light of temperature of the 50/50 Co<sub>3</sub>O<sub>4</sub>/CeO<sub>2</sub> catalyst is smaller than that of the 25/25/50 Ag<sub>2</sub>O/Co<sub>3</sub>O<sub>4</sub>/CeO<sub>2</sub> catalyst. The activity measurement showed that catalytic activity mostly depends on the physical properties of the catalysts and phases present in the structure. Addition of Ag<sub>2</sub>O to the Co<sub>3</sub>O<sub>4</sub>/CeO<sub>2</sub> catalysts lowered the activity. The pore volumes and average pore diameters of the catalysts decreased after Ag<sub>2</sub>O was added to the catalyst structure. The 50/50 Co<sub>3</sub>O<sub>4</sub>/CeO<sub>2</sub> catalyst calcined at 200 °C showed the best performance for the CO oxidation reaction.

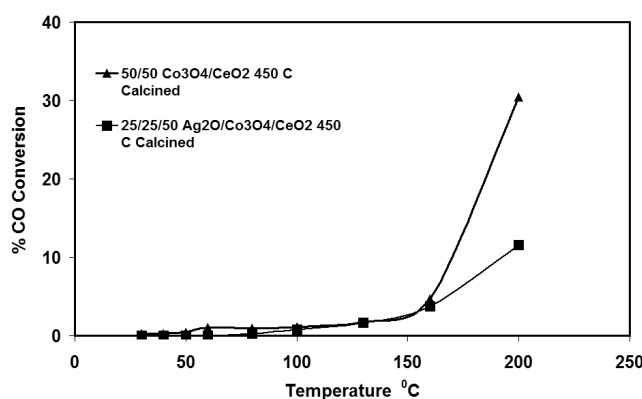


**Figure 4.** Catalytic activities of the catalysts as a function of temperature (1% CO, 21% O<sub>2</sub> and remaining He; S.V.: 45,000 h<sup>-1</sup>, 25-35 mg catalysts).

**Table 2.** CO conversion temperatures of the catalysts.

Catalysts	50% CO Conversion	100% CO Conversion
50/50 Co <sub>3</sub> O <sub>4</sub> /CeO <sub>2</sub>	122 °C	160 °C
25/25/50 Ag <sub>2</sub> O/Co <sub>3</sub> O <sub>4</sub> /CeO <sub>2</sub>	145 °C	200 °C

## Conclusion

The 100% Co<sub>3</sub>O<sub>4</sub>, 50/50 Co<sub>3</sub>O<sub>4</sub>/CeO<sub>2</sub>, and 25/25/50 Ag<sub>2</sub>O/Co<sub>3</sub>O<sub>4</sub>/CeO<sub>2</sub> catalysts were prepared and characterized. The effect of Ag<sub>2</sub>O and CeO<sub>2</sub> on the characteristic properties and CO oxidation activities of cobalt oxide based catalysts were investigated. X-ray diffraction studies showed that 50/50 Co<sub>3</sub>O<sub>4</sub>/CeO<sub>2</sub> and 25/25/50 Ag<sub>2</sub>O/Co<sub>3</sub>O<sub>4</sub>/CeO<sub>2</sub> catalysts have amorphous structures. Pore volumes and pore diameters were decreased by lowered cobalt oxide molar ratio and by the addition of Ag<sub>2</sub>O to the structure of the catalysts. The change in the properties of the catalysts affected the CO oxidation activity of the catalysts. The 50/50 Co<sub>3</sub>O<sub>4</sub>/CeO<sub>2</sub> catalysts were the most suitable catalysts for CO oxidation reaction after 150 °C reaction temperature.

## Acknowledgements

The authors gratefully acknowledge the financial support of the TÜBİTAK MISAG-229 and Gazi University BAP 06/2006-17 project.

## References

1. L.F. Liotta, G.D. Carlo, G. Pantaleo, A.M. Venezia and G. Deganello, **Appl. Catal. B- Environ.** **66**, 217 (2006).
2. D. Song and J. Li, **J. Mol. Catal. A- Chem.** **247**, 206 (2006).
3. N.O. Elbashir, P. Dutta, A. Manivannan, M.S. Seehra and C.B. Roberts, **Appl. Catal. A-Gen.** **285**, 169 (2005).
4. M. Luo, X. Yuan and X. Zheng, **Appl. Catal. A-Gen.** **175**, 121 (1998).
5. J. Jansson, A.E.C. Palmqvist, E. Fridell, M. Skoglundh, L. Österlund, P. Thormahlen and V. Langer, **J. Catal.** **211**, 387 (2002).
6. M. Kang, M.W. Song and C.H. Lee, **Appl. Catal. A-Gen.** **251**, 143 (2003).
7. P. Thormahlen, E. Fridell, N. Cruise, M. Skoglundh and A. Palmqvist, **Appl. Catal. B- Environ.** **31**, 1 (2001).
8. Ç. Güldür and F. Balıkçı, **Int. J. Hyd. Ener.** **27**, 219 (2002).
9. G.N. Salaita, Z.F. Hazos and G.B. Hoffund, **J. Elec. Spec. Rel. Phen.** **107**, 73 (2000).
10. A.I. Boronin, S.V. Koscheev, K.T. Murzakhmetov, V.I. Avdeev and G.M. Zhidomirov, **Appl. Surf. Sci.** **165**, 9 (2000).
11. G.I.N. Waterhouse, G.A. Bowmaker and J.B. Metson, **Appl. Surf. Sci.** **183**, 191 (2000).
12. D.V. Cesar, C.A. Perez, M. Schmal and V.M.M. Salim, **Appl. Surf. Sci.** **157**, 159 (2000).
13. H.A.E. Hagelin-Weaver, G.B. Hoffund, D.M. Minahan and G.N. Salaita, **Appl. Surf. Sci.** **235**, 420 (2004).
14. F. Larachi, J. Pierre, A. Adnot and A. Bernis, **Appl. Surf. Sci.** **195**, 236 (2002).
15. J.Z. Colina, R.M. Nix and H. Weiss, **Surf. Sci.** **563**, 251 (2004).
16. B. Skarman, D. Grandjean, R.E. Benfield, A. Hinz, A. Andersson and L.R. Wallenberg, **J. Catal.** **211**, 119 (2002).